Cage-based deformations for implicit surfaces

Kevin Trancho ⋆
Master 2 student in Computer sciences

at University Paris-Est Marne-la-Vallée
in Internship supervised by Loïc Barthe † and Pascal Romon ‡

June 21, 2019

⋆ | ⋆ † | ‡ | ⋆ † | ⋆ ‡

Topics of the presentation :

- Introduction to cage-based deformations.
  - Cages and interest as deformation.
  - Generalized barycentric coordinates in cages for deformation.
- How to deform an implicit surface with a cage.
  - Inverse position problem.
  - State of the art : Free-Form Deformations special type of cages and implicit surface deformation.
  - Our methods and flexible solving architecture.
- Future work and interest for Implicit skinning.

Cage on surface

- Bounding simplification of a discrete **surface**.
- Define **control positions**.
- Allow **smooth deformations** of the surface.

Cage on surface

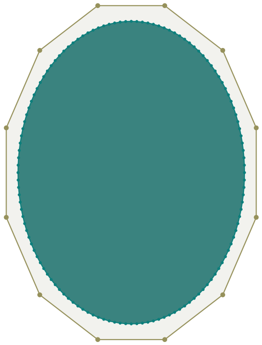

- Bounding simplification of a discrete **surface**.
- Define **control positions**.
- Allow **smooth deformations** of the surface.

Cage on surface

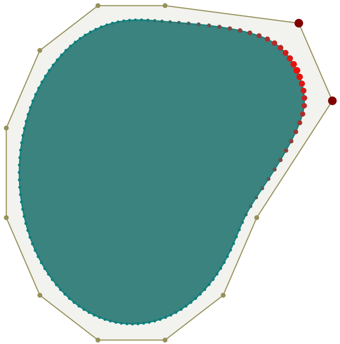

- Bounding simplification of a discrete **surface**.
- Define **control positions**.
- Allow **smooth deformations** of the surface.

Cage interest for animation

- Tool artists are familiar with.
- Allow smooth inside the cage and free deformations from control positions.
- Can be plug with a chosen barycentric coordinates system.
- Global space deformation.

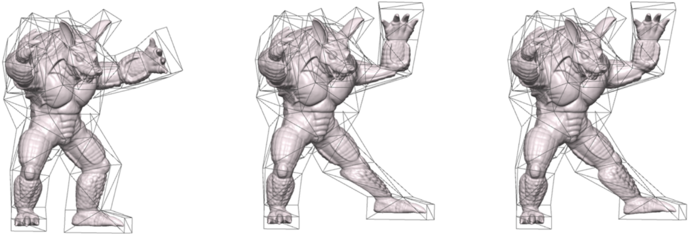

(a) Bind pose (b) Mean Value Coordinates (c) Green Coordinates

Barycentric coordinates and affine transform

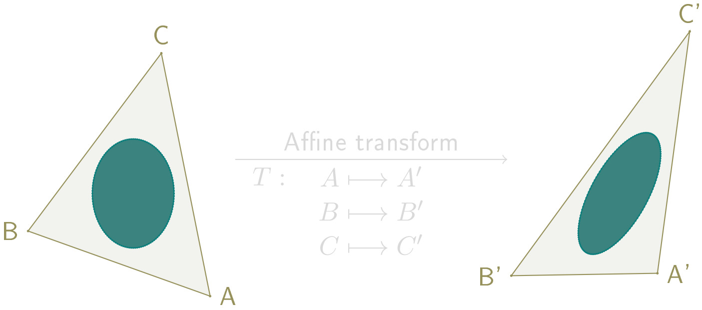

$$T: \quad A \longmapsto A'$$
$$B \longmapsto B'$$
$$C \longmapsto C'$$

$$P = \alpha A + \beta B + \gamma C$$
$$\alpha + \beta + \gamma = 1$$
$$\Rightarrow \alpha \vec{PA} + \beta \vec{PB} + \gamma \vec{PC} = 0$$

$$Q = T(P) = T(\alpha A + \beta B + \gamma C)$$
$$Q = \alpha T(A) + \beta T(B) + \gamma T(C)$$
$$Q = \alpha A' + \beta B' + \gamma C'$$

Barycentric coordinates and affine transform

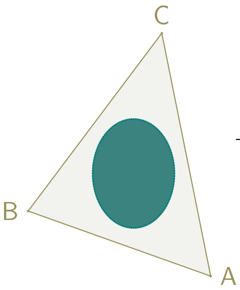

$$\xrightarrow{\text{Affine transform}}$$

$$T: \quad A \longmapsto A'$$
$$B \longmapsto B'$$
$$C \longmapsto C'$$

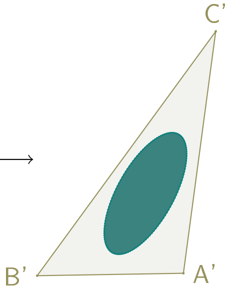

$$P = \alpha A + \beta B + \gamma C$$
$$\alpha + \beta + \gamma = 1$$
$$\Rightarrow \alpha \vec{PA} + \beta \vec{PB} + \gamma \vec{PC} = 0$$

$$Q = T(P) = T(\alpha A + \beta B + \gamma C)$$
$$Q = \alpha T(A) + \beta T(B) + \gamma T(C)$$
$$Q = \alpha A' + \beta B' + \gamma C'$$

Barycentric coordinates and affine transform

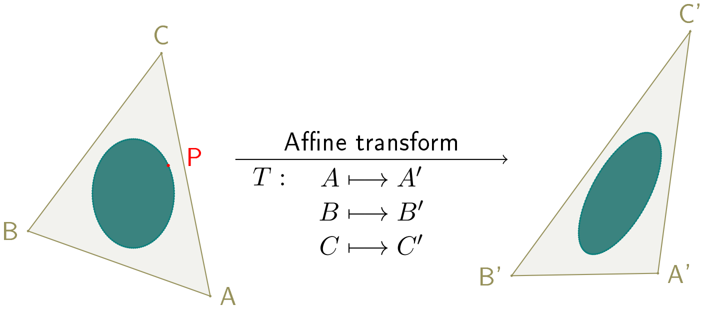

$$P = \alpha A + \beta B + \gamma C$$
$$\alpha + \beta + \gamma = 1$$
$$\Rightarrow \alpha \vec{PA} + \beta \vec{PB} + \gamma \vec{PC} = 0$$

$$Q = T(P) = T(\alpha A + \beta B + \gamma C)$$
$$Q = \alpha T(A) + \beta T(B) + \gamma T(C)$$
$$Q = \alpha A' + \beta B' + \gamma C'$$

Barycentric coordinates and affine transform

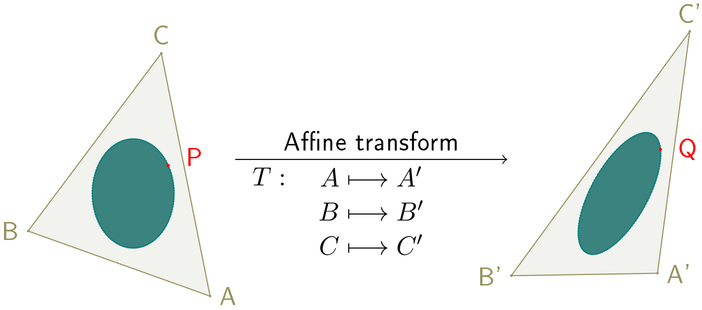

$$P = \alpha A + \beta B + \gamma C$$
$$\alpha + \beta + \gamma = 1$$
$$\Rightarrow \alpha \vec{PA} + \beta \vec{PB} + \gamma \vec{PC} = 0$$

$$Q = T(P) = T(\alpha A + \beta B + \gamma C)$$
$$Q = \alpha T(A) + \beta T(B) + \gamma T(C)$$
$$Q = \alpha A' + \beta B' + \gamma C'$$

Generalized barycentric coordinates to cages

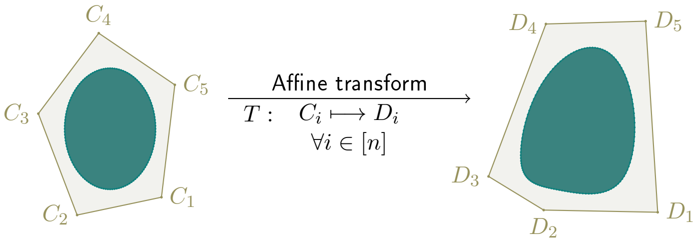

$$P = \sum_{i \in [n]} \alpha_i(P) C_i$$

$$\sum_{i \in [n]} \alpha_i(P) = 1$$

Binding step :
compute weights $(\alpha_i(P))_{i \in [n]}$

$$Q = T(P) = T\left(\sum_{i \in [n]} \alpha_i(P) C_i\right)$$

$$Q = \sum_{i \in [n]} \alpha_i(P) T(C_i)$$

$$Q = \sum_{i \in [n]} \alpha_i(P) D_i$$

Generalized barycentric coordinates to cages

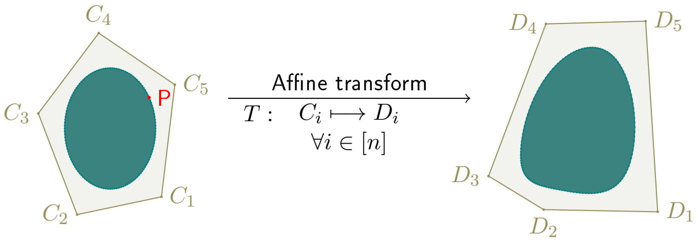

$$P = \sum_{i \in [n]} \alpha_i(P) C_i$$

$$\sum_{i \in [n]} \alpha_i(P) = 1$$

Binding step :

compute weights $(\alpha_i(P))_{i \in [n]}$

$$Q = T(P) = T(\sum_{i \in [n]} \alpha_i(P) C_i)$$

$$Q = \sum_{i \in [n]} \alpha_i(P) T(C_i)$$

$$Q = \sum_{i \in [n]} \alpha_i(P) D_i$$

Generalized barycentric coordinates to cages

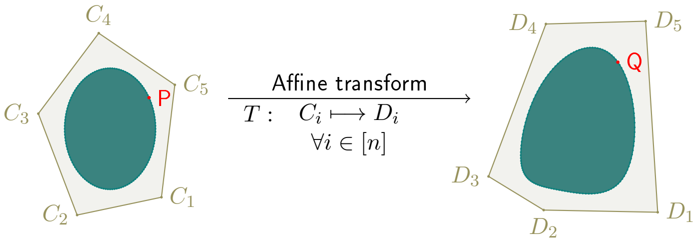

$$P = \sum_{i \in [n]} \alpha_i(P) C_i$$

$$\sum_{i \in [n]} \alpha_i(P) = 1$$

Binding step :
compute weights $(\alpha_i(P))_{i \in [n]}$

$$Q = T(P) = T(\sum_{i \in [n]} \alpha_i(P) C_i)$$

$$Q = \sum_{i \in [n]} \alpha_i(P) T(C_i)$$

$$Q = \sum_{i \in [n]} \alpha_i(P) D_i$$

Inverse position problem

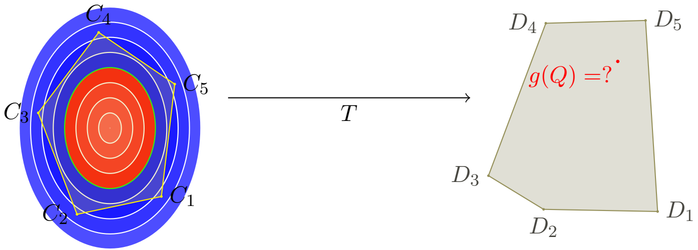

$$Q = \sum_{i \in [n]} \alpha_i(P)(C_i + \vec{u_i})$$

$$Q = P + \sum_{i \in [n]} \alpha_i(P)\vec{u_i}$$

$$g(Q) = f(P)$$

$$g(Q) = f(T^{-1}(Q))$$

$$Q = \sum_{i \in [n]} \alpha_i(P) D_i$$

$$P = Q - \sum_{i \in [n]} \alpha_i(P)\vec{u_i}$$

$\left\{\overrightarrow{C_1C_i}\right\}_{i \in [n] \setminus \{1\}}$ linearly dependent.

Inverse position problem

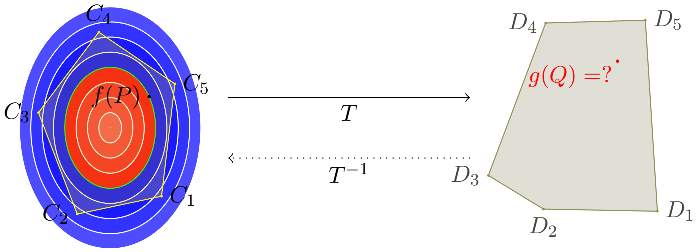

$$g(Q) = f(P)$$
$$g(Q) = f(T^{-1}(Q))$$
$$Q = \sum_{i\in[n]} \alpha_i(P)D_i$$

$$Q = \sum_{i\in[n]} \alpha_i(P)(C_i + \vec{u_i})$$
$$Q = P + \sum_{i\in[n]} \alpha_i(P)\vec{u_i}$$
$$P = Q - \sum_{i\in[n]} \alpha_i(P)\vec{u_i}$$

$\left\{\overrightarrow{C_1C_i}\right\}_{i\in[n]\setminus\{1\}}$ linearly dependent.

Inverse position problem

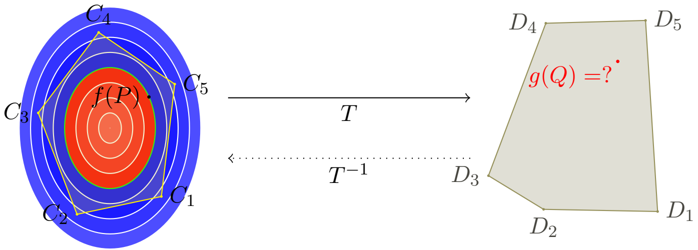

$$Q = \sum_{i \in [n]} \alpha_i(P)(C_i + \vec{u_i})$$

$$Q = P + \sum_{i \in [n]} \alpha_i(P)\vec{u_i}$$

$$P = Q - \sum_{i \in [n]} \alpha_i(P)\vec{u_i}$$

$$g(Q) = f(P)$$

$$g(Q) = f(T^{-1}(Q))$$

$$Q = \sum_{i \in [n]} \alpha_i(P) D_i$$

$\left\{\overrightarrow{C_1 C_i}\right\}_{i \in [n] \setminus \{1\}}$ linearly dependent.

Inverse position problem

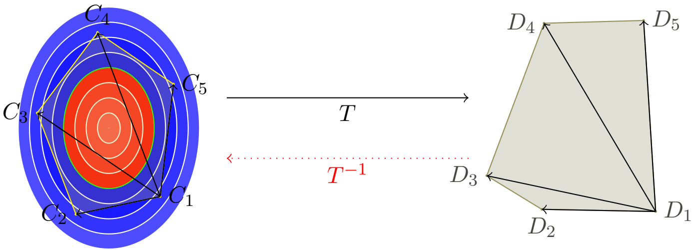

$$g(Q) = f(P)$$
$$g(Q) = f(T^{-1}(Q))$$
$$Q = \sum_{i \in [n]} \alpha_i(P) D_i$$

$$Q = \sum_{i \in [n]} \alpha_i(P)(C_i + \vec{u_i})$$
$$Q = P + \sum_{i \in [n]} \alpha_i(P)\vec{u_i}$$
$$\mathbf{P} = Q - \sum_{i \in [n]} \alpha_i(\mathbf{P})\vec{u_i}$$

$\left\{\overrightarrow{C_1 C_i}\right\}_{i \in [n] \setminus \{1\}}$ linearly dependent.

Free-Form-Deformations

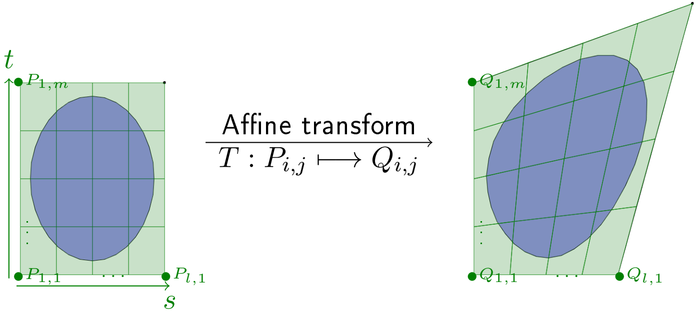

(s,t) coordinates in $(P_{1,1}, \overrightarrow{P_{1,1}P_{l,1}}, \overrightarrow{P_{1,1}P_{1,m}})$.
$P_{i,j}$ and $Q_{i,j}$ bilinear interpolation of the parallelepipeds.

$$T(s,t) = \sum_{(i,j)\in[l]\times[m]} \binom{l}{i}\binom{m}{j} s^i (1-s)^{l-i} t^j (1-t)^{m-j} T(P_{i,j})$$

Free-Form-Deformations and inverse problem solving

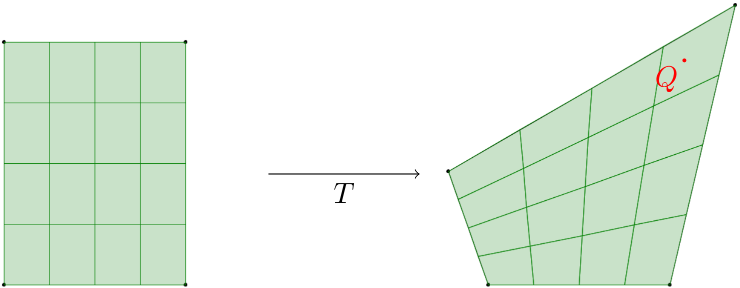

Get nearest $P_{i,j}$.
Solve $T(s,t) - Q = 0$
using Newton method.

$$J_T(s,t) = \left(\frac{\partial}{\partial s}T(s,t), \frac{\partial}{\partial t}T(s,t)\right)$$
$$X_0 = \left(\frac{i}{l}, \frac{j}{m}\right)$$
$$X_{n+1} = X_n - {J_T}^{-1}(X_n)\,(T(X_n) - Q)$$

Free-Form-Deformations and inverse problem solving

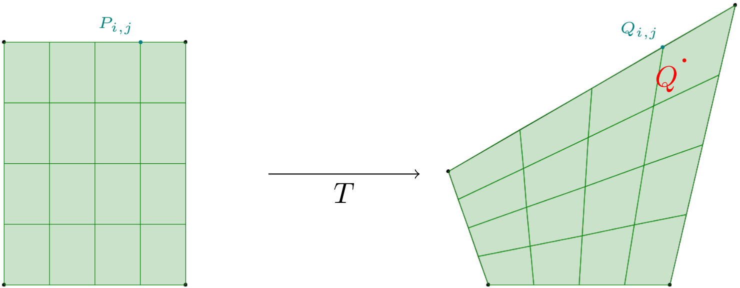

Get nearest $P_{i,j}$.
Solve $T(s,t) - Q = 0$
using Newton method.

$$J_T(s,t) = \left(\frac{\partial}{\partial s}T(s,t), \frac{\partial}{\partial t}T(s,t)\right)$$

$$X_0 = \left(\frac{i}{l}, \frac{j}{m}\right)$$

$$X_{n+1} = X_n - {J_T}^{-1}(X_n)\,(T(X_n) - Q)$$

Free-Form-Deformations and inverse problem solving

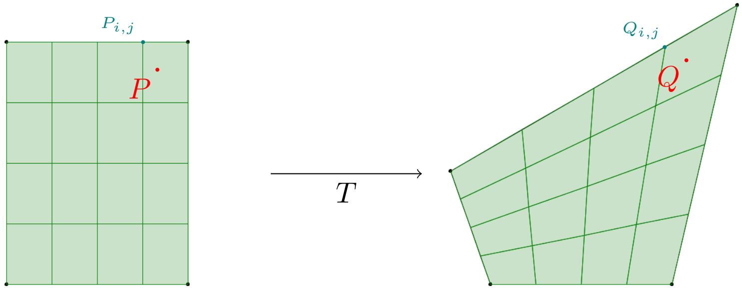

Get nearest $P_{i,j}$.
Solve $T(s,t) - Q = 0$
using Newton method.

$$J_T(s,t) = \left(\frac{\partial}{\partial s}T(s,t), \frac{\partial}{\partial t}T(s,t)\right)$$
$$X_0 = \left(\frac{i}{l}, \frac{j}{m}\right)$$
$$X_{n+1} = X_n - {J_T}^{-1}(X_n)\,(T(X_n) - Q)$$

Free-Form-Deformations implicit surface example in 2D

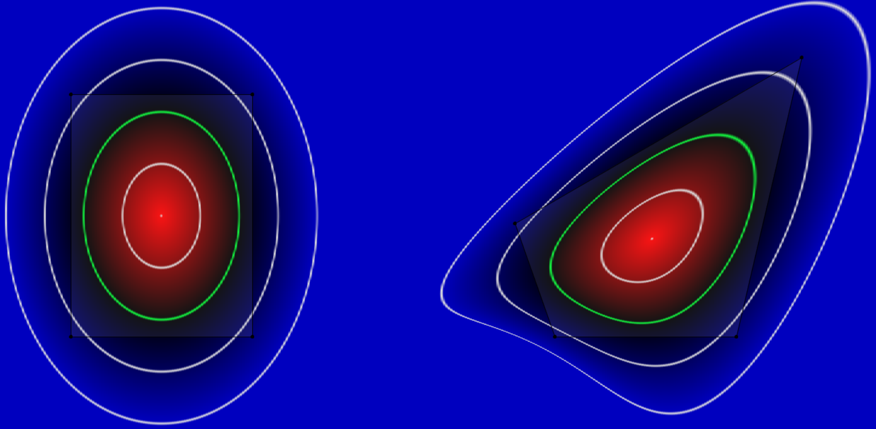

Example in 2D (render done in java using Processing IDE).

Our general architecture for inverse position solving

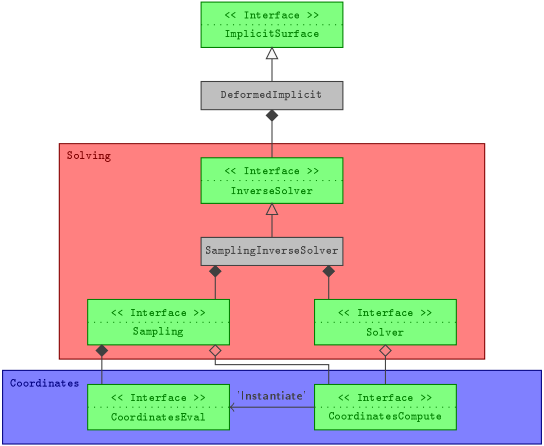

State of the art inspired idea : architecture

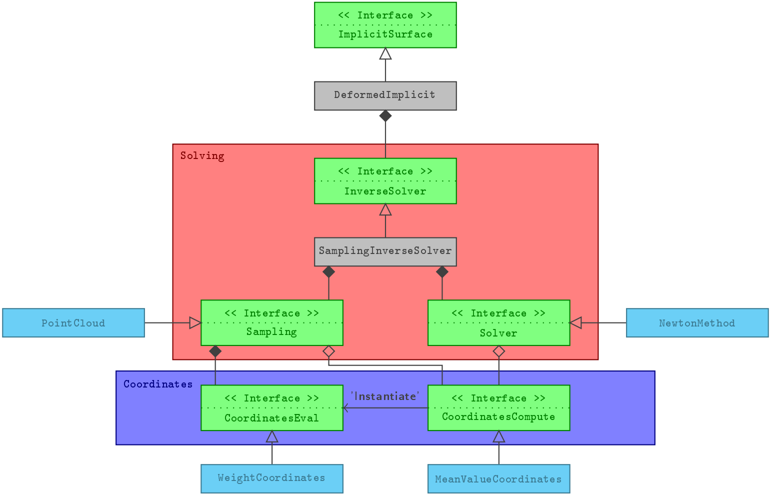

State of the art inspired idea : method

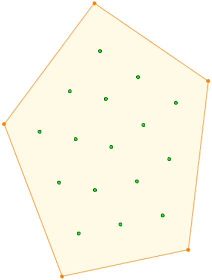

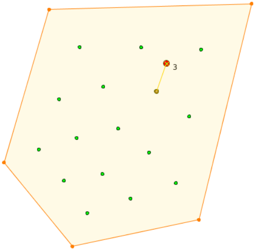

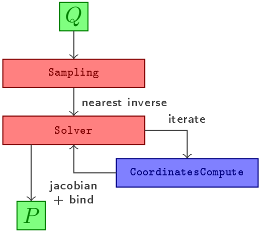

Solve $T(P) - Q = 0$:

$$J_T(x,y) = \left(\frac{\partial}{\partial x}T(x,y), \frac{\partial}{\partial y}T(x,y)\right)$$

P_0 nearest sample.

$$P_{n+1} = P_n - {J_T}^{-1}(P_n)\,(T(P_n) - Q)$$

State of the art inspired idea : method

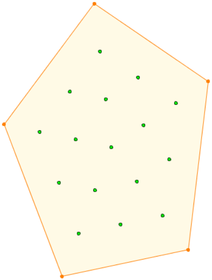

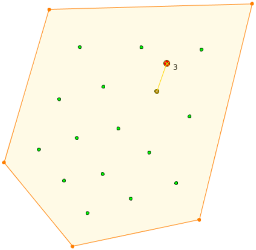

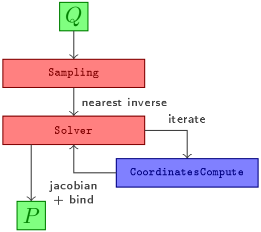

Solve $T(P) - Q = 0$:

$J_T(x, y) = \left(\frac{\partial}{\partial x} T(x, y), \frac{\partial}{\partial y} T(x, y)\right)$

P_0 nearest sample.

$P_{n+1} = P_n - {J_T}^{-1}(P_n)\,(T(P_n) - Q)$

State of the art inspired idea : result in 2D

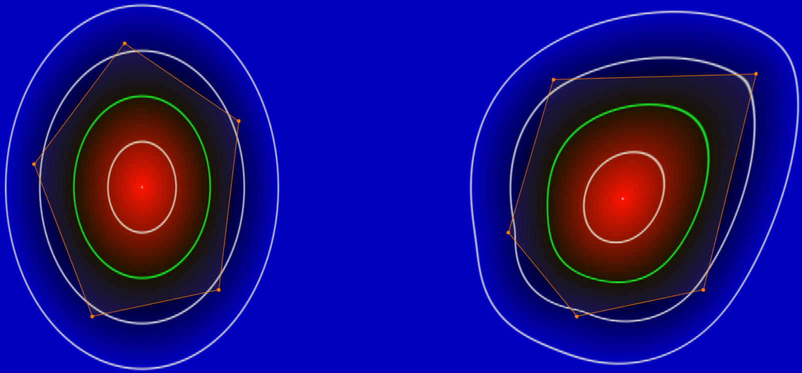

Example in 2D (render done in java using Processing IDE).

State of the art inspired idea : examples in 2D

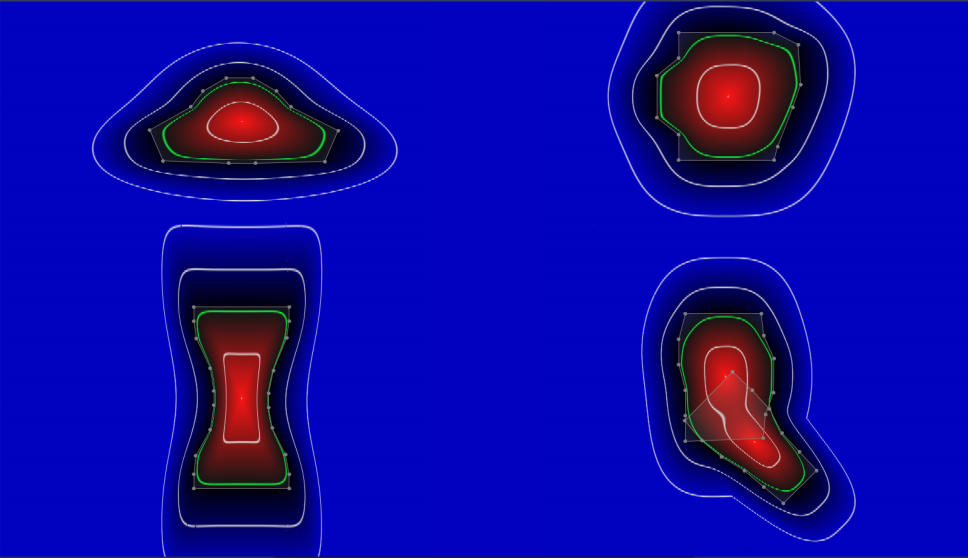

State of the art inspired idea : result in 3D

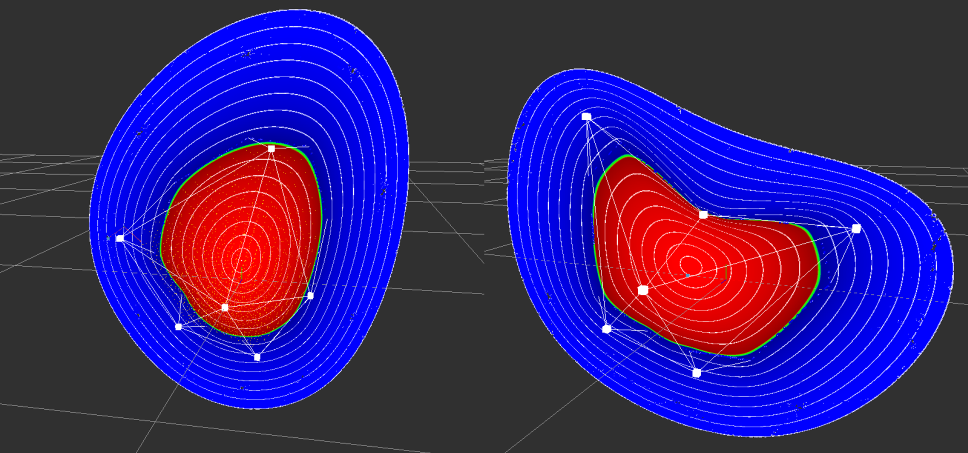

Example in 3D (render done in C++ using Radium Engine).

State of the art inspired : benchmark marching cubes

Implicit blob sphere deformed by cage (12 vertices, 20 faces) :

resolution	$16 \times 16 \times 16$ (2^{12})	$32 \times 32 \times 32$ (2^{15})	$64 \times 64 \times 64$ (2^{18})
time	$9.24 \cdot 10^8 ns (0.924s)$	$4.6 \cdot 10^9 ns (4.6s)$	$2.65 \cdot 10^{10} ns (26.5s)$
visualize	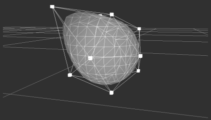	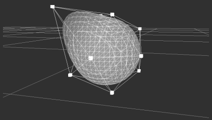	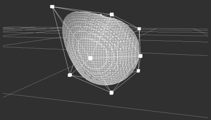

Kd-tree and sampling update time : $2.4 \cdot 10^6 ns (2.4ms)$ in average.

State of the art inspired : benchmark display planes

Implicit blob sphere deformed by cage (12 vertices, 20 faces) :

resolution	32×32 (2^{10})	128×128 (2^{14})	512×512 (2^{18})
time	$1.62 \cdot 10^8 ns (162ms)$	$2.4 \cdot 10^9 ns (2.4s)$	$3.82 \cdot 10^{10} ns (38.2s)$
visualize	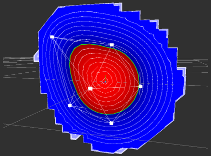	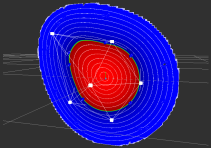	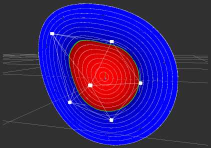

Kd-tree and sampling update time : $2.4 \cdot 10^6 ns (2.4ms)$ in average.

State of the art inspired idea : method

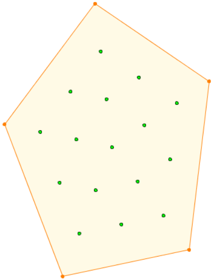

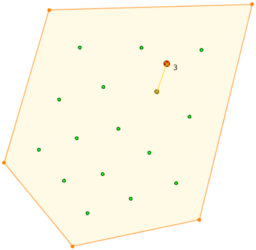

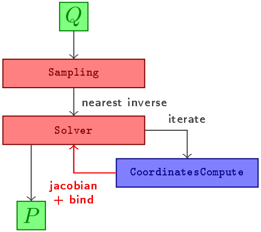

Solve $T(P) - Q = 0$:

$$J_T(x,y) = \left(\frac{\partial}{\partial x}T(x,y), \frac{\partial}{\partial y}T(x,y)\right)$$

P_0 nearest sample.

$$P_{n+1} = P_n - {J_T}^{-1}(P_n)\,(T(P_n) - Q)$$

Bounding grid and trilinear approximation : architecture

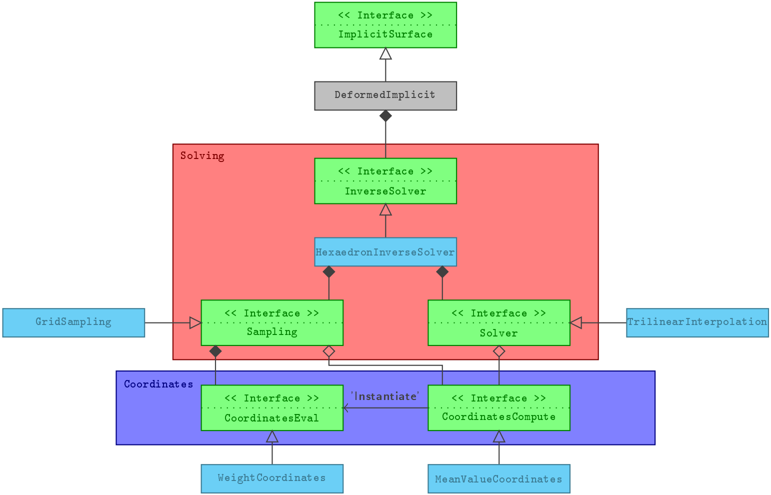

Bounding grid and trilinear approximation : method

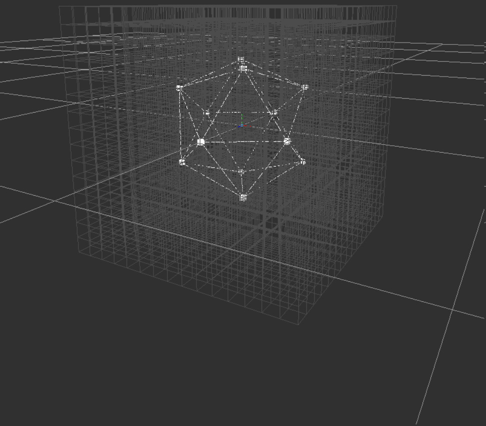

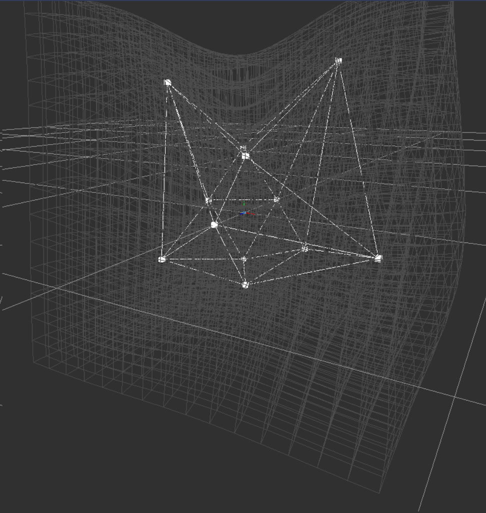

Bounding grid and trilinear approximation : method

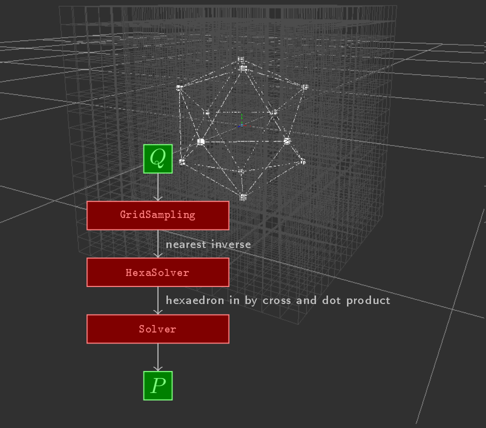

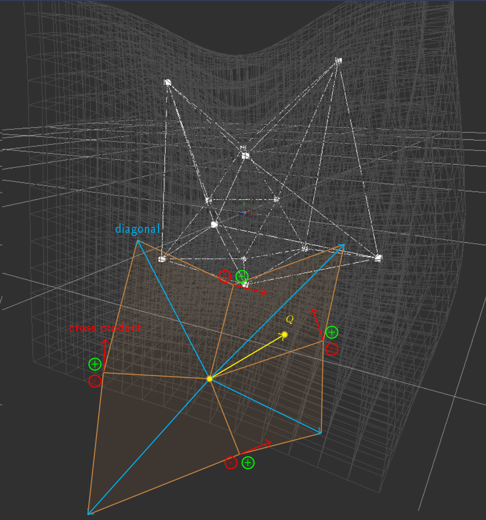

Bounding grid nearest neighbor : benchmark marching cubes

Implicit blob sphere deformed by cage (12 vertices, 20 faces) :

resolution	$16 \times 16 \times 16\ (2^{12})$	$32 \times 32 \times 32\ (2^{15})$	$64 \times 64 \times 64\ (2^{18})$
time	$9.9 \cdot 10^7 ns (99 ms)$	$4.1 \cdot 10^8 ns (410 ms)$	$1.8 \cdot 10^9 ns (1.8 s)$
visualize	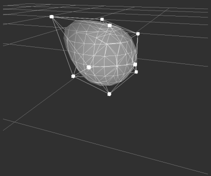	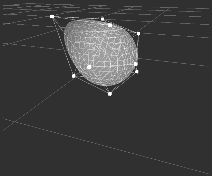	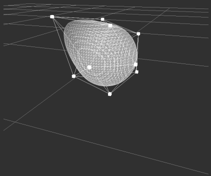

Kd-tree and sampling update time : $2.1 \cdot 10^7 ns (21 ms)$ in average.

Bounding grid nearest neighbor : benchmark display planes

Implicit blob sphere deformed by cage (12 vertices, 20 faces) :

resolution	32×32 (2^{10})	128×128 (2^{14})	512×512 (2^{18})
time	$7.9 \cdot 10^6 ns (7.9ms)$	$8 \cdot 10^7 ns (80ms)$	$1.29 \cdot 10^9 ns (1.29s)$
visualize	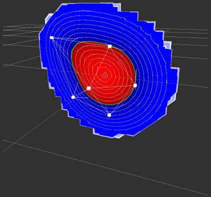	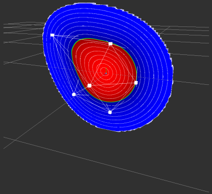	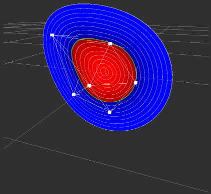

Kd-tree and sampling update time : $2.1 \cdot 10^7 ns (21ms)$ in average.

Bounding grid nearest neighbor : robustness to deforms problem

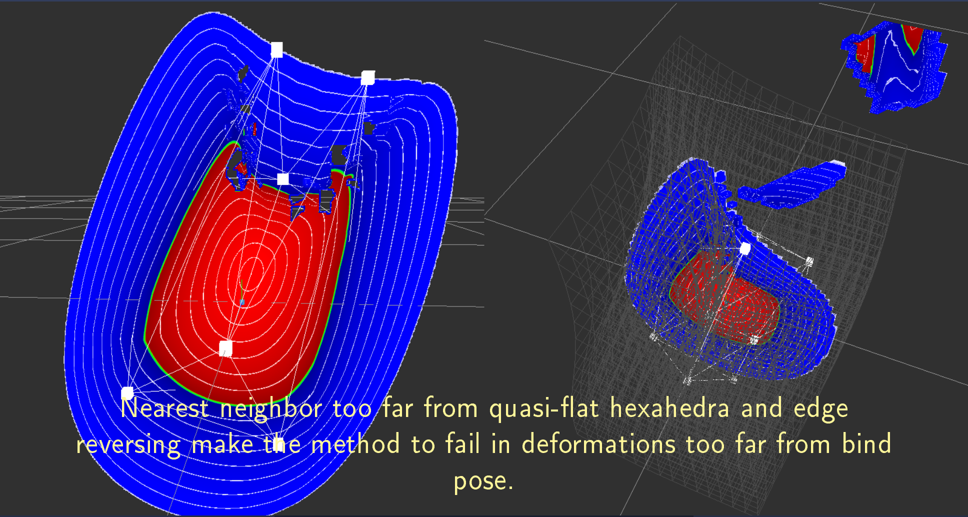

Nearest neighbor too far from quasi-flat hexahedra and edge reversing make the method to fail in deformations too far from bind pose.

Bounding grid tetrahedral cut : method

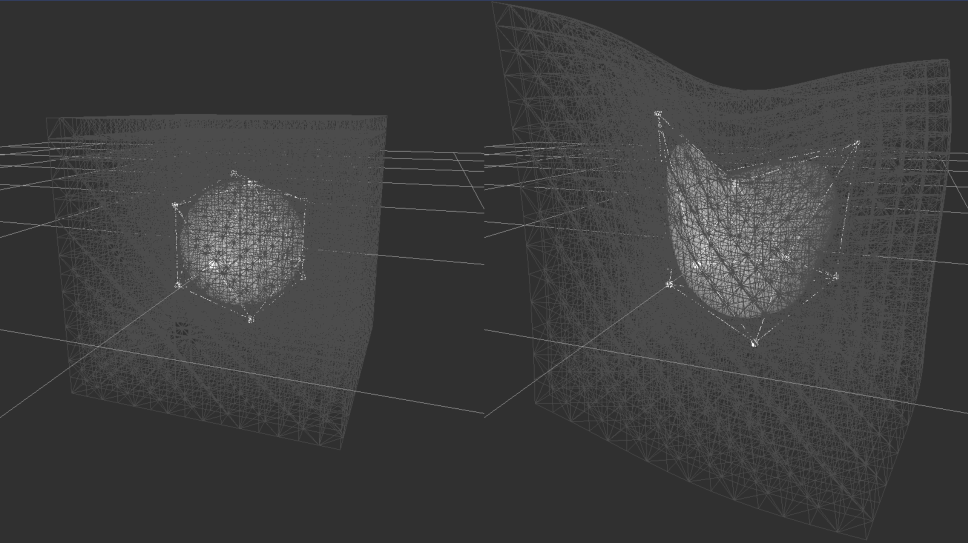

Bounding grid tetrahedral cut : method

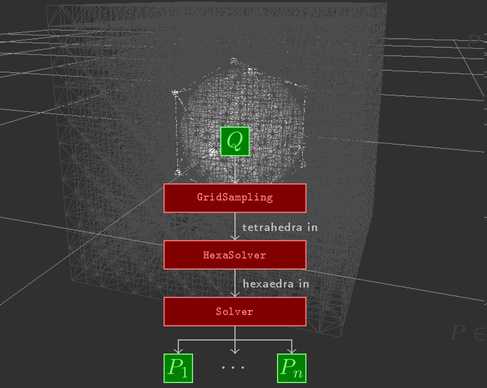

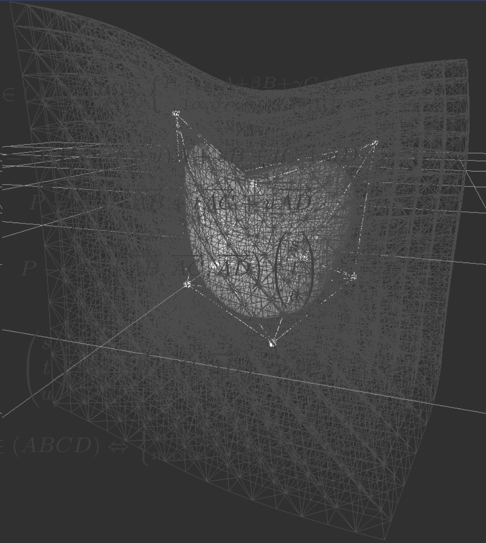

Bounding grid tetrahedral cut : method

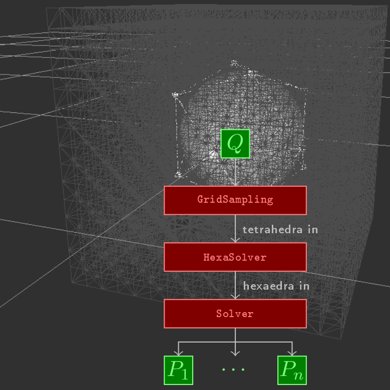

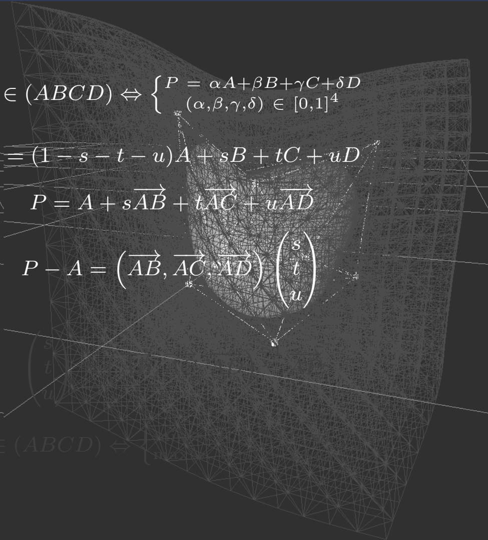

$$P \in (ABCD) \Leftrightarrow \begin{cases} P = \alpha A + \beta B + \gamma C + \delta D \\ (\alpha, \beta, \gamma, \delta) \in [0,1]^4 \end{cases}$$

$$P = (1 - s - t - u)A + sB + tC + uD$$

$$P = A + s\overrightarrow{AB} + t\overrightarrow{AC} + u\overrightarrow{AD}$$

$$P - A = \left(\overrightarrow{AB}, \overrightarrow{AC}, \overrightarrow{AD}\right) \begin{pmatrix} s \\ t \\ u \end{pmatrix}$$

Bounding grid tetrahedral cut : method

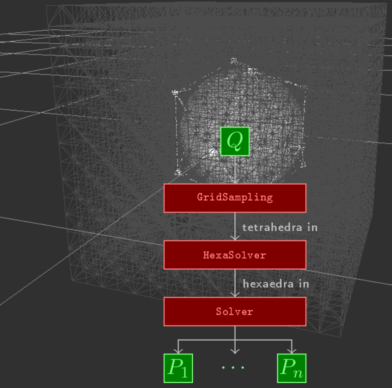

$$P \in (ABCD) \Leftrightarrow \begin{cases} P = \alpha A + \beta B + \gamma C + \delta D \\ (\alpha, \beta, \gamma, \delta) \in [0,1]^4 \end{cases}$$

$$P = (1 - s - t - u)A + sB + tC + uD$$

$$P = A + s\overrightarrow{AB} + t\overrightarrow{AC} + u\overrightarrow{AD}$$

$$P - A = \left(\overrightarrow{AB}, \overrightarrow{AC}, \overrightarrow{AD}\right) \begin{pmatrix} s \\ t \\ u \end{pmatrix}$$

$$\begin{pmatrix} s \\ t \\ u \end{pmatrix} = \left(\overrightarrow{AB}, \overrightarrow{AC}, \overrightarrow{AD}\right)^{-1} \overrightarrow{AP}$$

$$P \in (ABCD) \Leftrightarrow \begin{cases} \min(s,\ t,\ u,\ s+t+u) \geq 0 \\ \max(s,\ t,\ u,\ s+t+u) \leq 1 \end{cases}$$

Bounding grid tetrahedral cut : more robust solution

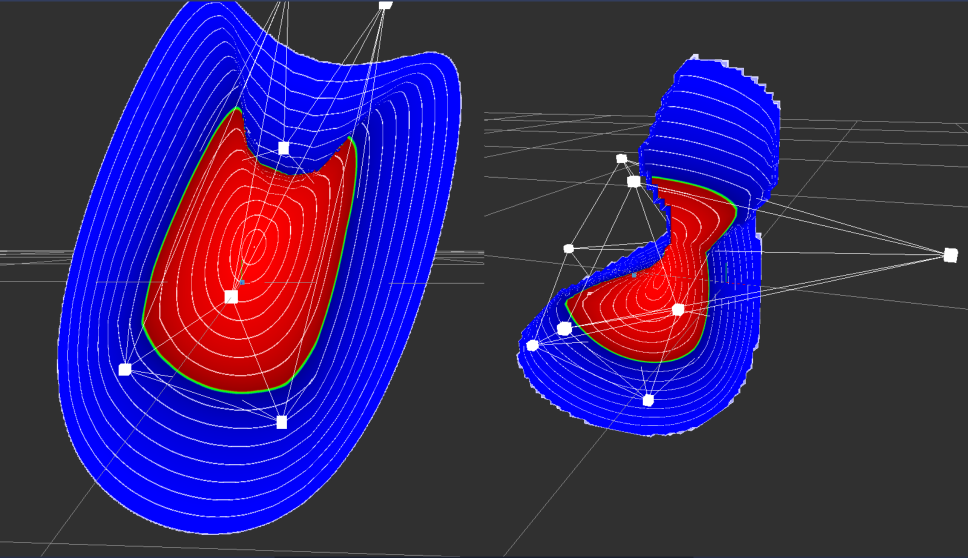

Bounding grid tetrahedral cut : benchmark marching cubes

Implicit blob sphere deformed by cage (12 vertices, 20 faces) :

resolution	$16 \times 16 \times 16$ (2^{12})	$32 \times 32 \times 32$ (2^{15})	$64 \times 64 \times 64$ (2^{18})
time	$8.5 \cdot 10^7 ns (85ms)$	$3.31 \cdot 10^8 ns (331ms)$	$1.37 \cdot 10^9 ns (1.37s)$
visualize	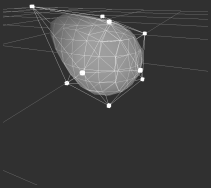	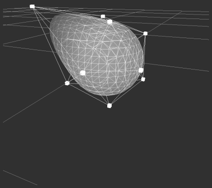	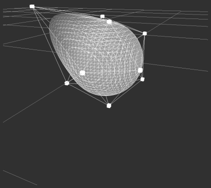

BIH and sampling update time : $1.7 \cdot 10^7 ns (17ms)$ in average.

Bounding grid tetrahedral cut : benchmark display planes

Implicit blob sphere deformed by cage (12 vertices, 20 faces) :

resolution	32×32 (2^{10})	128×128 (2^{14})	512×512 (2^{18})
time	$2.7 \cdot 10^7 ns (27ms)$	$6 \cdot 10^7 ns (60ms)$	$8.05 \cdot 10^8 ns (805ms)$
visualize			

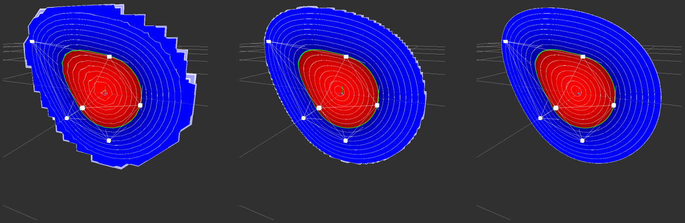

BIH and sampling update time : $1.7 \cdot 10^7 ns (17ms)$ in average.

Benchmark overview

Implicit blob sphere deformed by cage (12 vertices, 20 faces) :

Method :	State of the art inspired	Bounding grid nearest neighbor	Bounding grid tetrahedral cut
Update time	$2.4 \cdot 10^6 ns (2.4ms)$	$2.1 \cdot 10^7 ns (21ms)$	$1.7 \cdot 10^7 ns (17ms)$
Marching cubes :			
$16 \times 16 \times 16$ (2^{12})	$9.24 \cdot 10^8 ns (0.924s)$	$9.9 \cdot 10^7 ns (99ms)$	$8.5 \cdot 10^7 ns (85ms)$
$32 \times 32 \times 32$ (2^{15})	$4.6 \cdot 10^9 ns (4.6s)$	$4.1 \cdot 10^8 ns (410ms)$	$3.31 \cdot 10^8 ns (331ms)$
$64 \times 64 \times 64$ (2^{18})	$2.65 \cdot 10^{10} ns (26.5s)$	$1.8 \cdot 10^9 ns (1.8s)$	$1.37 \cdot 10^9 ns (1.37s)$
Display plane :			
32×32 (2^{10})	$1.62 \cdot 10^8 ns (162ms)$	$7.9 \cdot 10^6 ns (7.9ms)$	$2.7 \cdot 10^7 ns (27ms)$
128×128 (2^{14})	$2.4 \cdot 10^9 ns (2.4s)$	$8 \cdot 10^7 ns (80ms)$	$6 \cdot 10^7 ns (60ms)$
512×512 (2^{18})	$3.82 \cdot 10^{10} ns (38.2s)$	$1.29 \cdot 10^9 ns (1.29s)$	$8.05 \cdot 10^8 ns (805ms)$

Multiple equivalent self-intersection results

Implicit blob capsule deformed by cage (26 vertices, 48 faces) :

State of the art inspired
$1 \cdot 10^{11} ns (100s)$

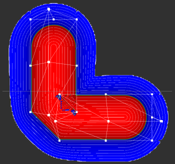

Bounding grid nearest neighbor
$1.4 \cdot 10^{9} ns (1.4s)$

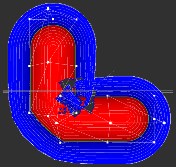

Bounding grid tetrahedral detection
$6.93 \cdot 10^{8} ns (693ms)$

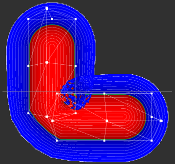

Bounding grid tetrahedral multiple detection
$7.17 \cdot 10^{8} ns (717ms)$

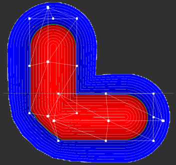

Multiple equivalent self-intersection results : zoom

Implicit blob capsule deformed by cage (26 vertices, 48 faces) :

State of the art inspired
$1 \cdot 10^{11} ns (100s)$

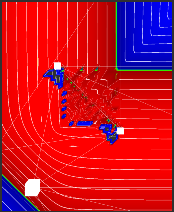

Bounding grid nearest neighbor
$1.4 \cdot 10^{9} ns (1.4s)$

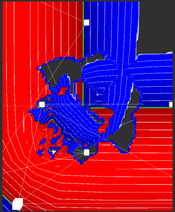

Bounding grid tetrahedral detection
$6.93 \cdot 10^{8} ns (693ms)$

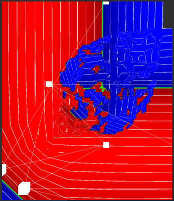

Bounding grid tetrahedral multiple detection
$7.17 \cdot 10^{8} ns (717ms)$

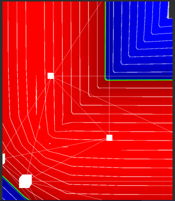

Multiple equivalent self-intersection and contact results

Implicit blob capsule deformed by cage (42 vertices, 80 faces) :

State of the art inspired
$1.58 \cdot 10^{11} ns (158s)$

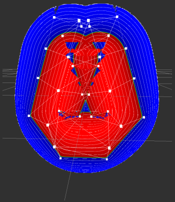

Bounding grid nearest neighbor
$2.2 \cdot 10^{9} ns (2.2s)$

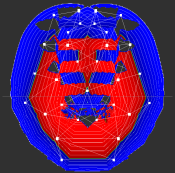

Bounding grid tetrahedral detection
$1.75 \cdot 10^{9} ns (1.75s)$

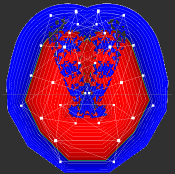

Bounding grid tetrahedral multiple detection
$1.67 \cdot 10^{9} ns (1.67s)$

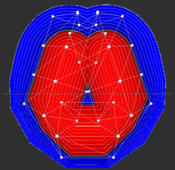

Space fold-over : movie time

Space fold-over solutions overview :

Bounding grid deform

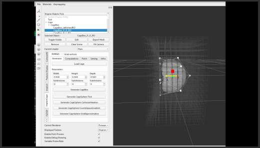

Bounding grid nearest neighbor

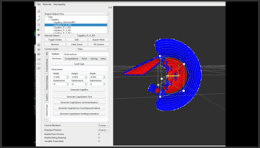

Bounding grid tetrahedral detection

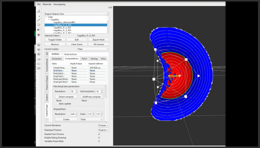

Bounding grid tetrahedral multiple detection solving (max)

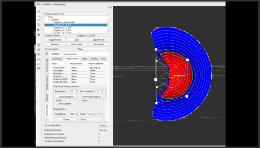

Bounding grid tetrahedral multiple detection solving (diff(max, min))

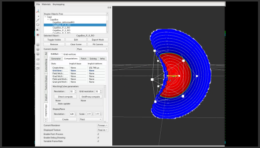

Bounding grid tetrahedral multiple and reversal detection solving (diff(space, reversed))

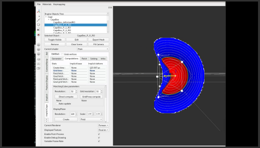

Improve continuity of the method

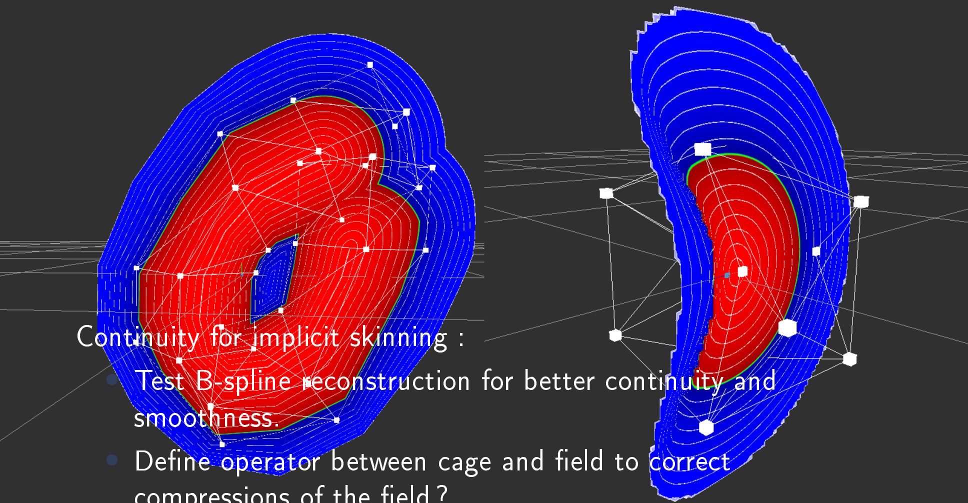

Continuity for implicit skinning :

- Test B-spline reconstruction for better continuity and smoothness.
- Define operator between cage and field to correct compressions of the field ?

Test Green and Local barycentric coordinates systems

Test other barycentric coordinates system :

- Green coordinates for quasi-conformal transform in 3D.

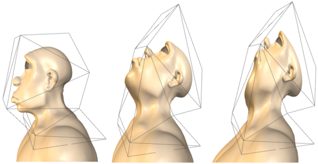

- Local barycentric coordinates for local transform of the space.

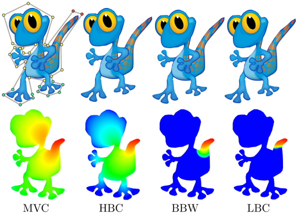

Integration to Implicit skinning

- Add smooth deformations.
- Allow free deformations for animators.

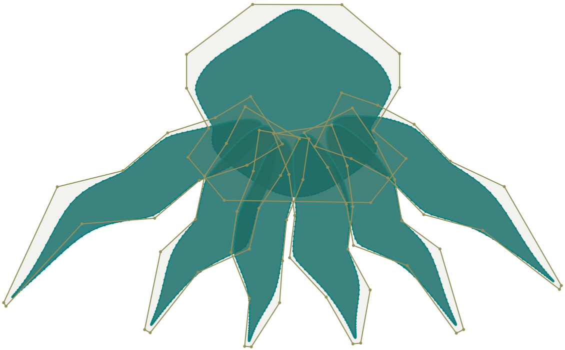

Correct mesh self-intersection

Case :	Self-contact	Self-intersection	...
Solution :	contact operator	skinning operator	
Visualize :			

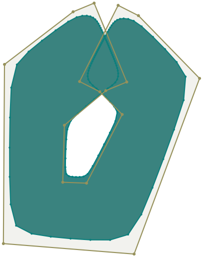

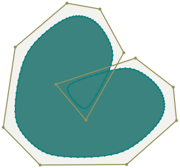

Conclusion

- Cages allow smooth and fast deformations we want to use to improve the Implicit skinning method.
- We propose a flexible plugin method to solve the inverse position problem and compute deformation of an implicit field.
- We are able to catch cases of multiple equivalents in original space to propose interesting solving of the implicit field in deformed space using composition operators.

Questions ?

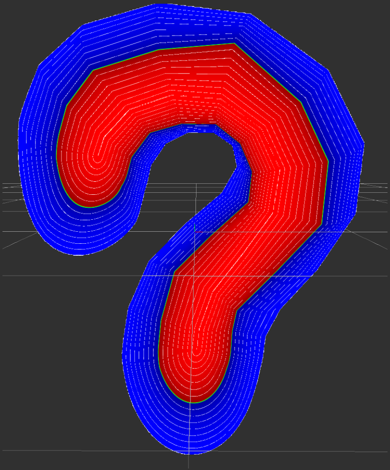

Student backup questions :

- Did you try other barycentric coordinates system in 2D ?
- Did you compute the gradient of MeanValueCoordinates in 2D ?
- Did you try other method to solve your time problem ?
- Can you show that barycentric coordinates through cages are linear with respect to affine transform ?

Green and MeanValue compare in 2d

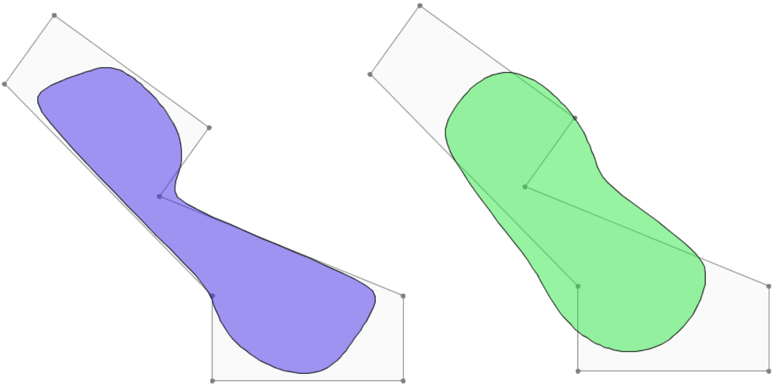

Green deform 2d

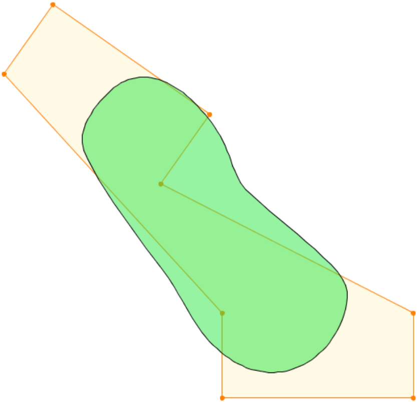

Green field 2d

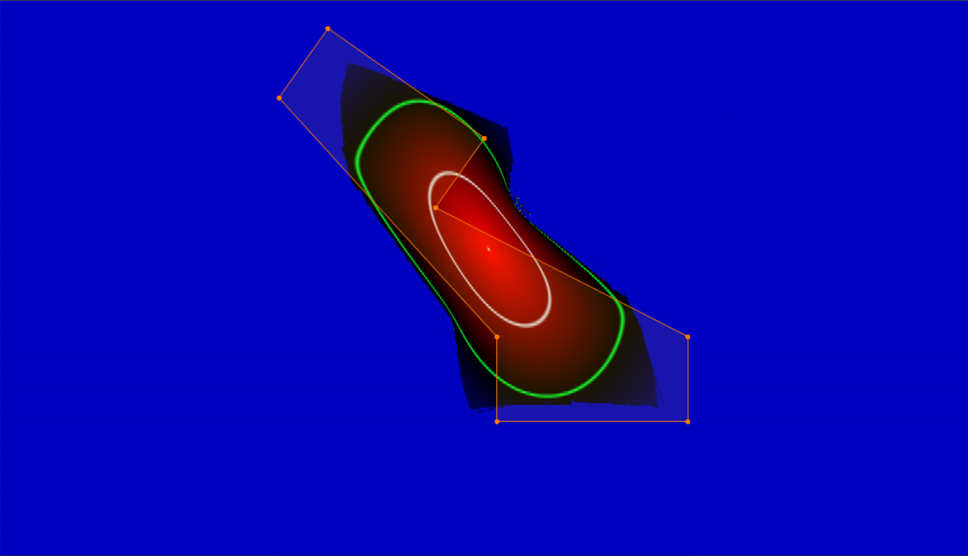

Using computed gradient : error

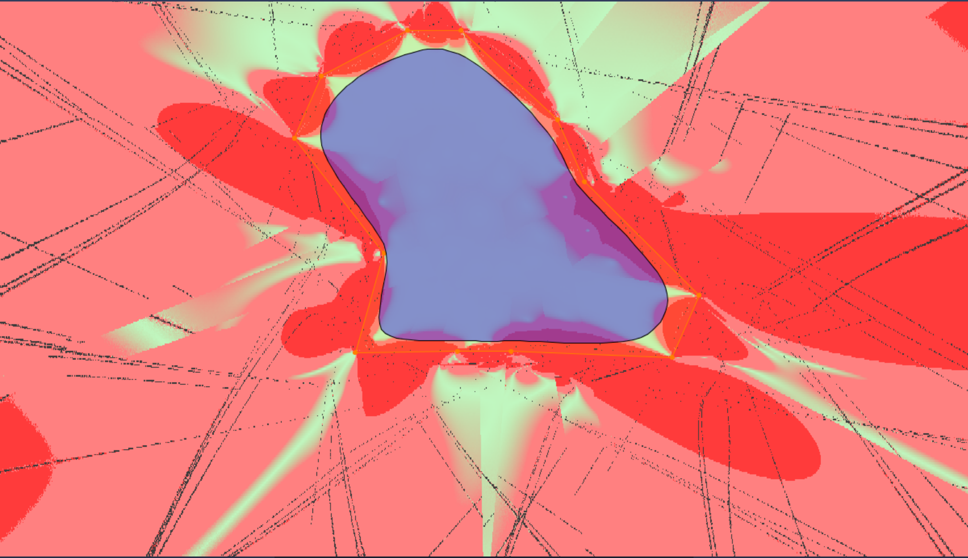

Using discrete gradient : error

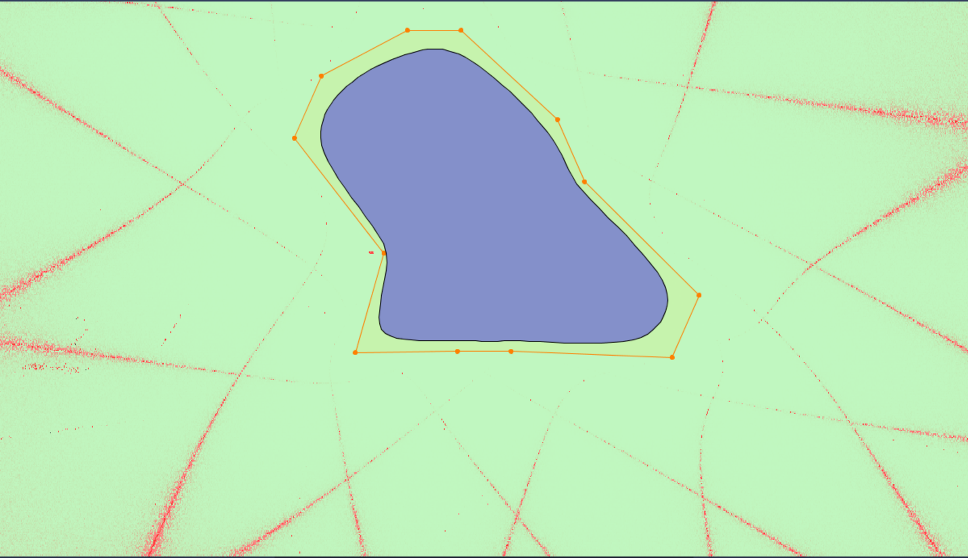

Using computed gradient : field

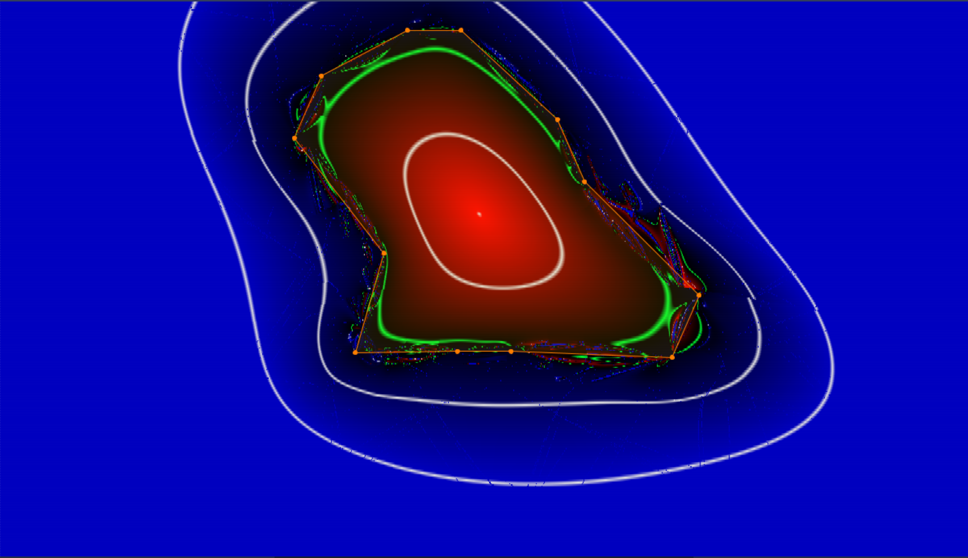

Using discrete gradient : field

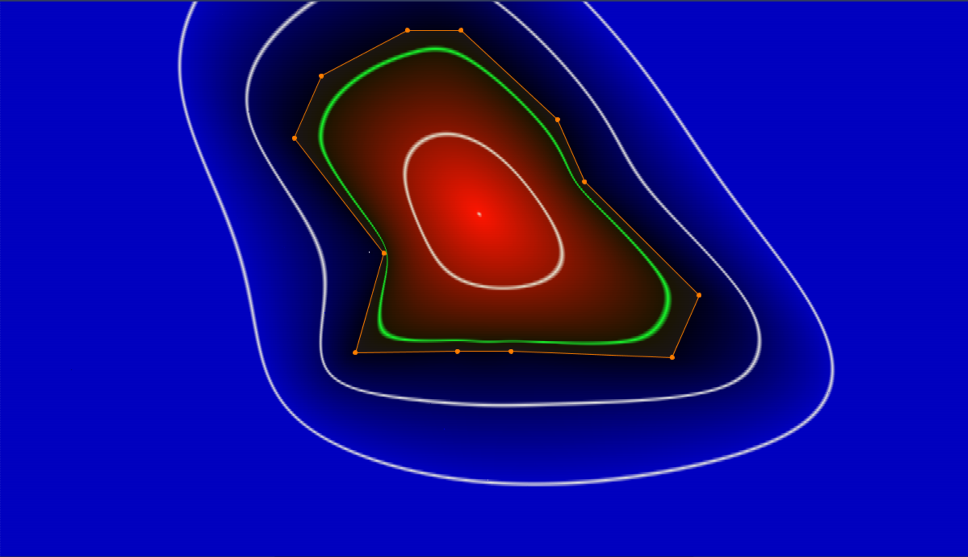

Using computed gradient : field without cage

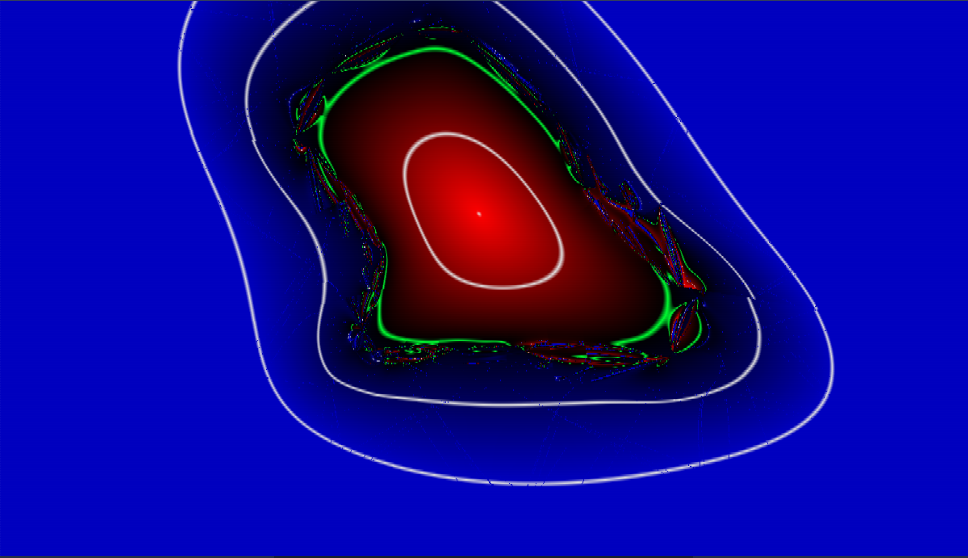

Using discrete gradient : field without cage

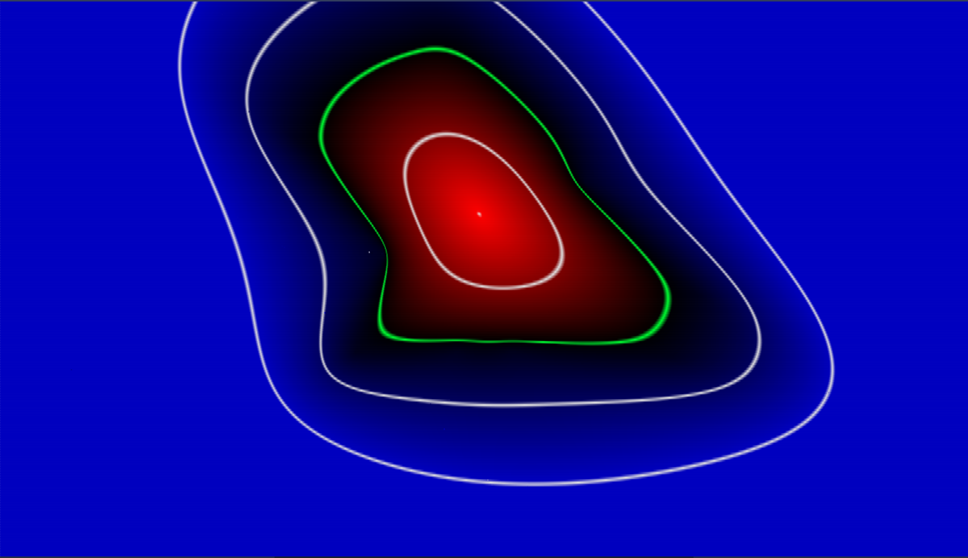

Gradient discontinuity on edges

$$a_i = C_i - P,\ b_i = C_{i+1} - P, \delta_i = \frac{a_i \cdot b_i}{||a_i||||b_i||}$$

$$\omega_i = \frac{\tan\left(\frac{\delta_{i-1}}{2}\right) + \tan\left(\frac{\delta_i}{2}\right)}{||a_i||},\ P = \frac{\sum\limits_{i\in[n]} \omega_i C_i}{\sum\limits_{i\in[n]} \omega_i}$$

$$\frac{\partial}{\partial\gamma}\delta_i = \frac{\partial}{\partial\gamma}\frac{a_i \cdot b_i}{||a_i||||b_i||} = (a_i \cdot b_i)\frac{a_{i,\gamma}||b_i||^2 + b_{i,\gamma}||a_i||^2}{||a_i||^3||b_i||^3} - \frac{a_{i,\gamma} + b_{i,\gamma}}{||a_i||||b_i||}$$

$$\frac{\partial}{\partial\gamma}\tan\left(\frac{\delta_i}{2}\right) = \frac{1 + \tan^2\left(\frac{\delta_i}{2}\right)}{2}\sqrt{\frac{||a_i||||b_i||}{||a_i||||b_i|| - a_i \cdot b_i}}\frac{\partial}{\partial\gamma}\delta_i$$

$$\frac{\partial}{\partial\gamma}\omega_i = \frac{\left(\frac{\partial}{\partial\gamma}\tan\left(\frac{\delta_{i-1}}{2}\right) + \frac{\partial}{\partial\gamma}\tan\left(\frac{\delta_i}{2}\right)\right)||a_i|| + \frac{a_{i,\gamma}}{||a_i||}\left(\tan\left(\frac{\delta_{i-1}}{2}\right) + \tan\left(\frac{\delta_i}{2}\right)\right)}{||a_i||^2}$$

$$\frac{\partial}{\partial\gamma}T(P) = \frac{\left(\sum \frac{\partial}{\partial\gamma}\omega_i T(C_i)\right)\left(\sum \omega_i\right) - \left(\sum \omega_i T(C_i)\right)\left(\sum \frac{\partial}{\partial\gamma}\omega_i\right)}{\left(\sum \omega_i\right)^2}$$

Gradient discontinuity on edges

$$a_i = C_i - P,\ b_i = C_{i+1} - P, \delta_i = \frac{a_i \cdot b_i}{||a_i||||b_i||}$$

$$\omega_i = \frac{\tan\left(\frac{\delta_{i-1}}{2}\right) + \tan\left(\frac{\delta_i}{2}\right)}{||a_i||},\ P = \frac{\sum\limits_{i\in[n]} \omega_i C_i}{\sum\limits_{i\in[n]} \omega_i}$$

$$\frac{\partial}{\partial\gamma}\delta_i = \frac{\partial}{\partial\gamma}\frac{a_i \cdot b_i}{||a_i||||b_i||} = (a_i \cdot b_i)\frac{a_{i,\gamma}||b_i||^2 + b_{i,\gamma}||a_i||^2}{||a_i||^3||b_i||^3} - \frac{a_{i,\gamma} + b_{i,\gamma}}{||a_i||||b_i||}$$

$$\frac{\partial}{\partial\gamma}\tan\left(\frac{\delta_i}{2}\right) = \frac{1 + \tan^2\left(\frac{\delta_i}{2}\right)}{2}\sqrt{\frac{||a_i||||b_i||}{||a_i||||b_i|| - a_i \cdot b_i}}\frac{\partial}{\partial\gamma}\delta_i$$

$$\frac{\partial}{\partial\gamma}\omega_i = \frac{\left(\frac{\partial}{\partial\gamma}\tan\left(\frac{\delta_{i-1}}{2}\right) + \frac{\partial}{\partial\gamma}\tan\left(\frac{\delta_i}{2}\right)\right)||a_i|| + \frac{a_{i,\gamma}}{||a_i||}\left(\tan\left(\frac{\delta_{i-1}}{2}\right) + \tan\left(\frac{\delta_i}{2}\right)\right)}{||a_i||^2}$$

$$\frac{\partial}{\partial\gamma}T(P) = \frac{\left(\sum \frac{\partial}{\partial\gamma}\omega_i T(C_i)\right)\left(\sum \omega_i\right) - \left(\sum \omega_i T(C_i)\right)\left(\sum \frac{\partial}{\partial\gamma}\omega_i\right)}{\left(\sum \omega_i\right)^2}$$

Gradient descent in Coordinates space

Minimize $||\sum_{i\in[n]} \alpha_i T(C_i) - Q||^2$.

$$\frac{\partial}{\partial \alpha_k}||\sum_{i\in[n]} \alpha_i T(C_i) - Q||^2 = 2T(C_k) \cdot \left(\sum_{i\in[n]} \alpha_i T(C_i) - Q\right)$$

$$\nabla||\sum_{i\in[n]} \alpha_i T(C_i) - Q||^2 = 2 \quad {}^t\left(T(C_1), T(C_2), \ldots, T(C_n)\right) \cdot \left(\sum_{i\in[n]} \alpha_i T(C_i) - Q\right)$$

Do gradient descent.

Coordinates space gradient descent : result

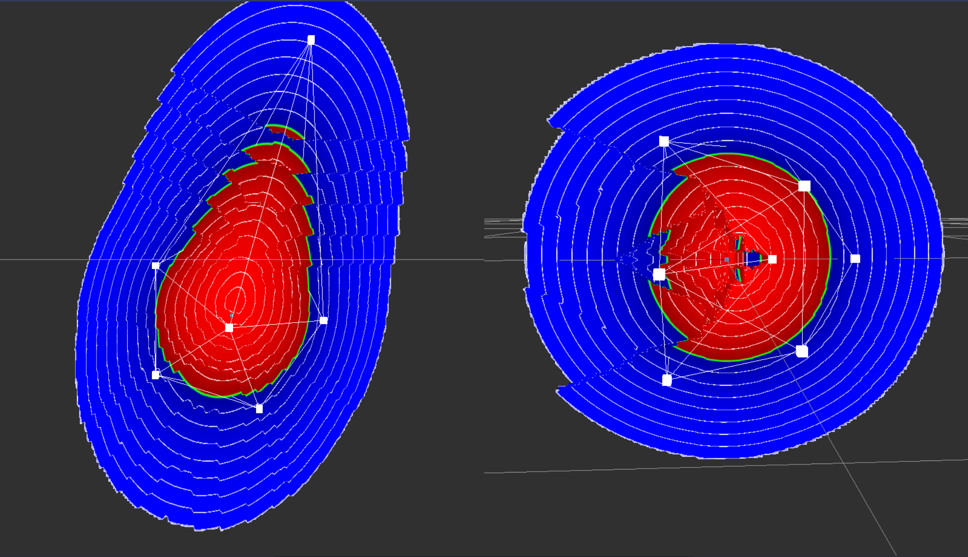

Coordinates space gradient descent : benchmark display planes

Implicit blob sphere deformed by cage (12 vertices, 20 faces) :

resolution	32×32 (2^{10})	128×128 (2^{14})	512×512 (2^{18})
time	$1 \cdot 10^7 ns (10ms)$	$1.58 \cdot 10^8 ns (158ms)$	$2.4 \cdot 10^9 ns (2.4s)$
visualize	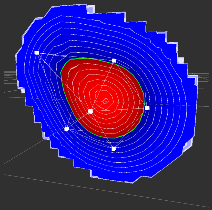	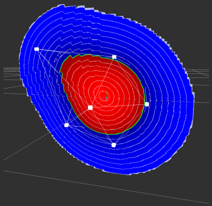	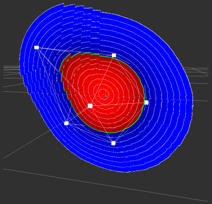

Gradient descent in Coordinates space

Find $\{\mathfrak{C}_j\}_{j \in [l]}$ orthonormal basis of constraints from coordinates system.
Then do gradient descent on :

$$\nabla_{\mathfrak{C}} || \sum_{i \in [n]} \alpha_i T(C_i) - Q||^2 = \nabla || \sum_{i \in [n]} \alpha_i T(C_i) - Q||^2 - \sum_{j \in [l]} \frac{\nabla || \sum_{i \in [n]} \alpha_i T(C_i) - Q||^2 \cdot \mathfrak{C}_j}{\mathfrak{C}_j \cdot \mathfrak{C}_j} \mathfrak{C}_j$$

- Is constraints computation that relevant for time saving ?
- Nearest neighbor's like method : no multiple equivalent solving.
- Benchmark times near to Bounding grid methods.